

# Density of electronic states in density-wave compounds with imperfect nesting

A. V. Tsvetkova,<sup>1</sup> Ya. I. Rodionov,<sup>2</sup> and P. D. Grigoriev<sup>2</sup>

<sup>1</sup>*National University of Science and Technology MISIS, Moscow, 119049 Russia*

<sup>2</sup>*Institute for Theoretical and Applied Electrodynamics,  
Russian Academy of Sciences, Moscow, 125412 Russia*

(Dated: January 3, 2025)

We study the effects of imperfect nesting in a simple 2D tight-binding model on the electronic properties in the density-wave (DW) state. The discussed model reflects the main features of quasi-1D metals where the DW emerges. We show that an imperfect nesting leads to unusual singularities in the quasi-particle density of states, leading to a strong renormalization of the superconducting critical temperature. We also compute the conductivity tensor of the normal state and obtain a satisfactory agreement with the experimental data on rare-earth tritellurides and many other DW materials.

PACS numbers: 72.10.-d, 72.15.Gd, 71.55.Ak, 72.80.-r

## I. INTRODUCTION

The interplay between superconductivity (SC) and charge or spin density wave (DW) attracts a vast research activity. The SC-DW competition and coexistence appears in various strongly-correlated electron systems, including the high-temperature cuprate [1–6] and iron-based [7–10] superconductors, NbSe<sub>2</sub> [11–13] and other rare-earth di- and poly-chalcogenides [14, 15], various organic superconductors [16–24], and many other materials (see, e.g., Refs. [25–27] for reviews).

The DW in metals creates a spatial modulation of the charge or spin density of conducting electrons with the wave vector  $\mathbf{Q}$  and opens a gap  $\Delta_0$  on the Fermi level in the electronic spectrum, which lowers the electron energy [28]. Depending on the electron dispersion  $\epsilon(\mathbf{k})$  in this metal, two different DW states are possible. The first one, called the perfect nesting of the Fermi surface (FS), happens when  $\epsilon(\mathbf{k}) + \epsilon(\mathbf{k} + \mathbf{Q}) < \Delta_0$  for all  $\mathbf{k}$  at the FS. Then the DW covers the entire FS and the metal becomes a semiconductor in a DW state. In this case a uniform SC on a DW background is hardly possible, but SC may appear via a spatial segregation with DW, as happens in various materials [22, 24, 29–31]. This SC heterogeneity can be visualized by the scanning tunneling microscopy (STM) and spectroscopy [29, 32–40], by the local diamagnetic probe [41, 42], or detected and analyzed using the resistivity anisotropy measurements [43–48]. The spatial DW-SC phase segregation usually appears on a large length scale, greater than the DW coherence length  $\xi_{DW} = \hbar v_F / (\pi \Delta)$ , as it happens in organic superconductors [22, 24, 47], or on the microscopic scale, i.e. in the form of DW soliton walls [49–51].

The second scenario of DW-SC coexistence appears in the case of imperfect FS nesting when  $\epsilon(\mathbf{k}) + \epsilon(\mathbf{k} + \mathbf{Q}) > \Delta_0$  for some  $\mathbf{k}$  at the FS. In this case the metallic conductivity survives in a DW state till  $T \rightarrow 0$ , being anisotropically reduced, e.g., as in various rare-earth three-chalcogenides [52] and many other materials [25–28]. One could expect an exponential decrease of the superconducting transition temperature  $T_c$  on the DW

background even in the imperfect-nesting case, because according to the BCS theory in the weak-coupling regime

$$T_c \sim \omega_D \exp(-1/g\nu_F) \quad (1)$$

exponentially depends on the electron density of states (DoS) at the Fermi level  $\nu_F$  multiplied by the coupling constant  $g$ , with the Debye frequency  $\omega_D$  in the pre-exponential factor. As the DW opens a gap at least on some parts of FS, the DoS  $\nu_F$  is reduced by the DW, leading to a destructive SC-DW interference [53, 54]. However, usually, one has a more complicated SC-DW interplay: the superconducting transition temperature  $T_c$  is the highest at the quantum critical point (QCP) where the density wave (DW) gets suppressed by some external parameter, such as doping level [1–6], pressure [7–10, 16–22], cooling rate [23, 24], disorder [12], etc. The  $T_c$  dome-like shape near the DW QCP results from the enhancement of electron-electron (e-e) interaction  $g \rightarrow g_*(\mathbf{Q})$  in the Cooper channel by the critical DW fluctuations, which can be described as the SC vertex renormalization in the language of Feynman diagram technique [55, 56]. Note that this vertex renormalization changes its momentum dependence and may favor the unconventional superconductivity [57–59].

Below we consider only the second scenario of the uniform DW in the case of imperfect nesting. What is stronger, the SC coupling renormalization  $g \rightarrow g_*(\mathbf{Q})$  or the DoS reduction  $\nu_F \rightarrow \nu_{F*}$  by the DW? This question is very important for the SC transition temperature in the weak-coupling regime given by Eq. (1). According to the theoretical calculations [55–58] the SC coupling enhancement  $g \rightarrow g_*(\mathbf{Q})$  is not very strong, especially far from the DW QCP, when the DW order parameter  $\Delta$  is larger than the SC energy gap. On the contrary, the gapped FS area in the DW state is, usually, rather large, as visualized by ARPES measurements in various compounds [60–70]. How the observed increase of  $T_c$  on the DW background, implying the increase of the product  $g\nu_F$ , is then possible?

The insight resolving this apparent inconsistency is proposed in Ref. [71] where the electronic DoS in the

DW state with slightly imperfect nesting is calculated in the mean-field approximation and shown to be unexpectedly large at the Fermi level even if the ungapped FS pockets are very small. This happens because of the strong renormalization of electron spectrum by the DW. Hence,  $T_c$  on the DW background, taking into account the coupling-constant renormalization  $g \rightarrow g_*(\mathbf{Q})$ , can be even larger than the SC transition temperature  $T_{c0}$  without DW. The calculations in Ref. [71] are limited by the very small ungapped FS pockets and are performed under some approximations about the electron dispersion.

In this paper we generalize these calculations of the DoS on the DW background for the case of arbitrary imperfect nesting, when the size of ungapped FS parts may be large. Although the main goal of our calculations is to estimate the change of SC transition temperature by the DW background, our results are useful also for other electronic properties of DW compounds, even without superconductivity. For example, the DoS enters the electronic part of specific heat and other thermodynamic and transport electron properties, which can be measured.

## II. MODEL

The DW state usually appears in strongly anisotropic quasi-1D metals because of their good FS nesting [27, 28, 72]. In many other DW compounds there is a hidden quasi-one-dimensionality, although their electronic transport exhibits a 2D isotropy along the conducting layers. An example of such a hidden quasi-1D electron spectrum are the rare-earth tritellurides [52, 73] or tetratellurides [74, 75], where the FS consists of two pairs of perpendicular quasi-1D warped sheets originating from the Te  $p_x$  and  $p_y$  orbitals, giving almost tetragonal symmetry of electronic properties, broken by the CDW [52]. Of course, there are some DW materials with closed quasi-2D rather than open quasi-1D FS, but even they have some nearly flat FS parts, such as transition metal dichalcogenides [76] or high- $T_c$  cuprates [66, 77]. Below we consider quasi-1D metals as a quite generic system bearing the DW.

In layered quasi-2D metals due to crystal periodicity the electron dispersion is given by the Fourier series

$$\varepsilon(\mathbf{k}) = -2t_x \cos(ak_x) - 2t_y \cos(bk_y) - \sum_{i,j \geq 2} 2t_{ij} \cos(ak_x i) \cos(bk_y j), \quad (2)$$

where  $a$  and  $b$  are the lattice constants in  $x$  and  $y$  directions. The tunneling amplitude along the  $z$  axis is considerably smaller than that along the conducting layers  $x, y$  and is discarded, as it does not play any role in the analysis below. Usually, the last term in Eq. (2) is much smaller than the first two and is also omitted, corresponding to the tight-binding model [78, 79].

In quasi-1D metals, where the  $x$ -axis represents an easy-conducting chain direction and  $t_x \gg t_y$ , it is often

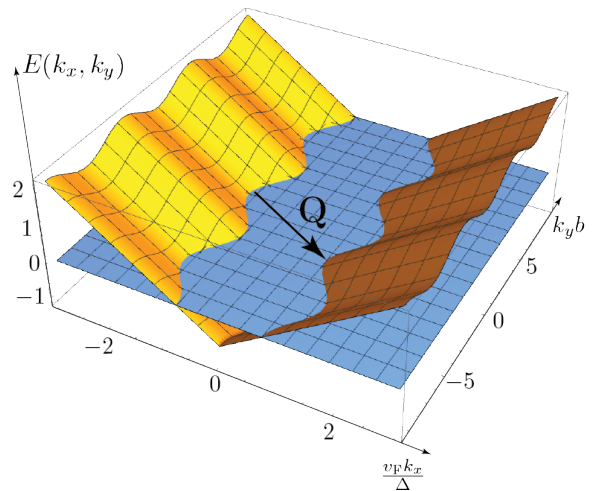


FIG. 1. The electron spectrum  $E(k_x, k_y)$  given by Eq. (3) and shown by yellow surface. The FS (two Fermi wavy curves in the  $k_x - k_y$  plane) is formed by the intersection of this spectrum with the horizontal plane of fixed electron energy equal to the chemical potential or Fermi energy.

convenient to linearize the  $k_x$  electron dispersion near the Fermi level. Then the free-electron dispersion without magnetic field can be written as [27, 71, 80, 81]

$$\varepsilon(\mathbf{k}) = v_F(|k_x| - k_F) - 2t_y \cos(bk_y) - 2t'_y \cos(2bk_y), \quad (3)$$

where  $b$  is the lattice constant in  $y$  direction and the first term represents the electron dispersion along the  $x$ -direction linearized near the Fermi surface. Even if all  $t_{ij} = 0$  in Eq. (2),  $t'_y \sim t_y^2/t_x \neq 0$  and comes from the nonlinearity of electron dispersion along the  $x$ -direction. We drop all the other hopping amplitudes in  $y$ -direction, as they are small by the parameter  $t_y/t_x \ll 1$ .

Without the last *antinessing*  $t'_y$  term in Eq. (3) the perfect nesting condition

$$\varepsilon(\mathbf{k}) + \varepsilon(\mathbf{k} + \mathbf{Q}) = 0 \quad (4)$$

is satisfied at wave vector  $\mathbf{Q} = (2k_F, \pi/b)$  (see Fig. 1). The electron spectra and FS near  $k_F$  and  $-k_F$  are nested with the nesting vector  $\mathbf{Q}$ . The outlined quasi-1D system exhibits the charge-density wave (CDW) formation as the result of a nesting-driven Fermi surface instability. This leads to the opening of gap  $\Delta$  in the quasiparticle spectrum. However, this simple picture undergoes a dramatic change once we take into account the antinessing amplitude  $t'_y$ .

Although in quasi-1D metals  $t'_y \sim t_y^2/t_x \ll t_y$ , the retained term  $t'_y$  rather than  $t_y$  competes with the energy gap  $\Delta$  in the resulting ground state equations. The  $2t'_y$  term in (3) is called “antinessing” because it violates the nesting condition (4). In what follows, we discard the possible influence of  $t'_y$  on the nesting vector  $\mathbf{Q}$  and discuss the legitimacy of this approach in section IV.

As seen from Fig. (1), the FS consists of two warped unconnected curves separated by vector  $\mathbf{Q}$ . This allows to us to split the quasiparticle Fock's space into two disconnected parts corresponding to the neighborhood of each Fermi sheet

$$\begin{aligned}\psi(\mathbf{r}) &= \sum_{\mathbf{k} \in U(\mathbf{k}_F)} a(\mathbf{k})e^{i\mathbf{k}\mathbf{r}} + \sum_{\mathbf{k} \in U(-\mathbf{k}_F)} a(\mathbf{k})e^{i\mathbf{k}\mathbf{r}} \\ &\equiv \sum_{\mathbf{k}} a_1(\mathbf{k})e^{i\mathbf{k}\mathbf{r}} + \sum_{\mathbf{k}} a_2(\mathbf{k})e^{-i\mathbf{k}\mathbf{r}}\end{aligned}\quad (5)$$

As usually in Peierls's transition physics, we assume that the deformation of the lattice has a static nature. The lattice deformation potential mixes two different parts (see Eq. (5)) of the Fock's space and adds one more term in the Hamiltonian. Accordingly, the electron Hamiltonian can be written as follows

$$\hat{H} = \hat{H}_0 + \hat{H}_{\text{int}} \quad (6)$$

with the free-electron part in momentum representation being

$$\hat{H}_0 = \sum_{\mathbf{k}} a_1^\dagger(\mathbf{k})a_1(\mathbf{k})\varepsilon(\mathbf{k}) + \sum_{\mathbf{k}} a_2^\dagger(\mathbf{k})a_2(\mathbf{k})\varepsilon(\mathbf{Q} + \mathbf{k}). \quad (7)$$

and the electron-lattice interaction part given by

$$\hat{H}_{\text{int}} = \Delta \sum_{\mathbf{k}} \left( a_1(\mathbf{k})a_2^\dagger(\mathbf{k}) + a_1^\dagger(\mathbf{k})a_2(\mathbf{k}) \right), \quad (8)$$

where  $\Delta$  is proportional to the amplitude of lattice deformation. In the physics of the Peierls transition  $\Delta \equiv \Delta(T)$  becomes the temperature-dependent gap of the quasiparticle spectrum.

Diagonalization of the Hamiltonian (6) leads to the standard gapped spectrum

$$E(\mathbf{k}) = \frac{\varepsilon(\mathbf{k}) + \varepsilon(\mathbf{k} + \mathbf{Q})}{2} \pm \sqrt{\frac{(\varepsilon(\mathbf{k}) - \varepsilon(\mathbf{k} + \mathbf{Q}))^2}{4} + \Delta^2}. \quad (9)$$

Substituting Eq. (3) to Eq. (9) we obtain the following quasiparticle spectrum in the presence of the CDW

$$E(k_x, k_y) = -2t'_y \cos 2k_y \pm \sqrt{(k_x v_F - t_y \cos k_y)^2 + \Delta^2}. \quad (10)$$

We illustrate this quasiparticle spectrum in Fig. (2).

### III. CALCULATIONS AND RESULTS

#### A. Quasiparticle DOS

To understand the behavior of the transport properties of the system we need to compute the single particle density of states (DOS)

$$\nu(\varepsilon) = \sum_{\mathbf{k}} \delta(\varepsilon - E(\mathbf{k})) \equiv \int \delta(\varepsilon - E(\mathbf{k})) \frac{dk_x dk_y}{(2\pi)^2}, \quad (11)$$

where  $\delta(x)$  is the Dirac  $\delta$ -function. Integration is performed over the Brillouin zone. Due to the symmetry of gapped spectrum (9) the integration region can be reduced to the quarter of the Brillouin zone. After the integration over  $q_x$  the expression (11) becomes

$$\nu(\varepsilon) = \frac{1}{\pi^2 v_F} \int_0^{\pi/2} \frac{|\varepsilon + \Delta_1 \cos 2q_y b|}{\sqrt{(\varepsilon + \Delta_1 \cos 2q_y b)^2 - \Delta^2}} dq_y \quad (12)$$

with the notation  $\Delta_1 \equiv 2t'_y$  introduced for convenience. Although the integral (12) can only be evaluated numerically (see Fig. 3), one can obtain analytical results in some regions where the DOS reveals intriguing (singular) behavior. These cases are discussed in the next subsection.

#### B. The behavior of DOS near singularities

The DOS is an even function of energy as can be easily checked from expression (12). This function has two singularities. The jump at point  $\Delta_1 - \Delta$  and the divergence at point  $\Delta_1 + \Delta$  correspond to the appearance and the merger of the closed pockets on the surface of fixed energy (see Fig. 2).

The singularities in the DOS are seen from the structure of the integrand in Eq. (12). Namely, we see that the square root in the denominator of the integrand of (12) has the branch points at energy  $\varepsilon = \Delta \pm \Delta_1$  where the pockets of the constant energy surface start to merge, as in Fig. (2) (b). The corresponding analytical expression for the DOS near the threshold energy  $\Delta + \Delta_1$  reads:

$$\begin{aligned}\nu(\Delta + \Delta_1 + \delta\varepsilon) &= \frac{1}{\pi^2 v_F b} \left[ 2 \arcsin \sqrt{\frac{\Delta_1}{\Delta + \Delta_1}} \right. \\ &\quad \left. + \sqrt{\frac{\Delta}{4\Delta_1}} \left( \ln \frac{32\Delta}{\Delta_1 + \Delta} - \ln \frac{\delta\varepsilon}{\Delta_1} \right) \right].\end{aligned}\quad (13)$$

As we see from Eq. (13), the DOS has a logarithmic singularity at the threshold energy  $\varepsilon = \Delta + \Delta_1$ , where it coincides with the sum of the CDW gap  $\Delta$  and the antineesting parameter  $\Delta_1$ . This corrects and generalizes the qualitative analysis presented in Ref. [71] (Fig. 3), where the log-singularity was predicted at  $\varepsilon = \Delta$  instead of  $\Delta + \Delta_1$ .

There exists another threshold  $\varepsilon = \Delta_1 - \Delta$ . We need to address two possible situations:  $\Delta < \Delta_1$  and  $\Delta > \Delta_1$ . We have the following results for the DOS (see Appendix

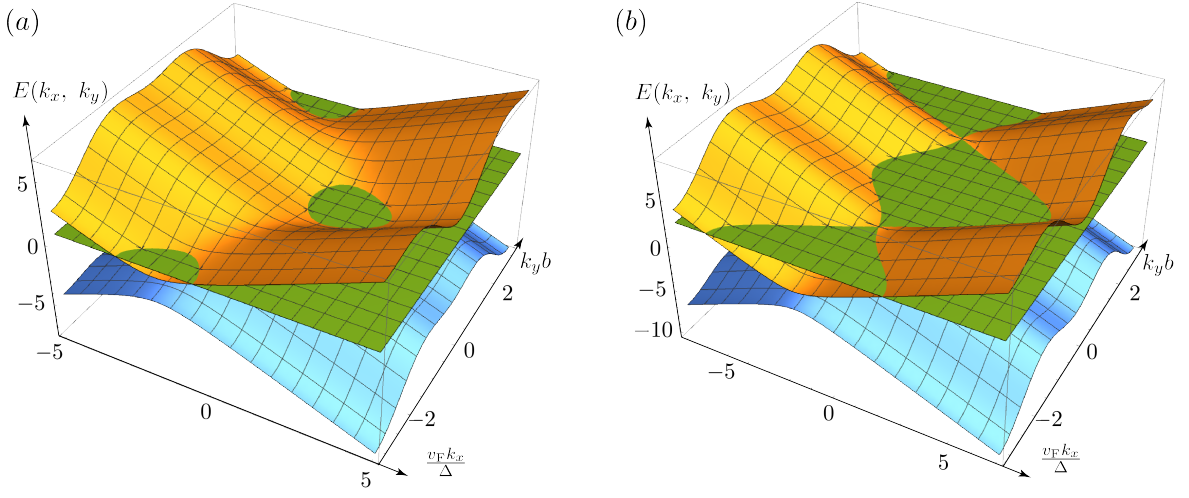


FIG. 2. (a) The quasiparticle spectrum (yellow) in the presence of a CDW with  $\Delta_1 = 0.8\Delta$ . The green plane corresponds to the constant energy cross section  $\varepsilon = \Delta_1 \equiv 2t'_y$ . The closed pockets are clearly seen as green puddles above the yellow surface. (b) The spectrum of the quasiparticles in the presence of the CDW. The green plane corresponds to the position of the constant energy cross section, the antinesting  $\Delta_1 = 1.5\Delta$  and the energy level  $\varepsilon = \Delta + \Delta_1$ , where  $\Delta$  is the Peierls energy gap. The critical energy at which the DOS manifests log divergence.

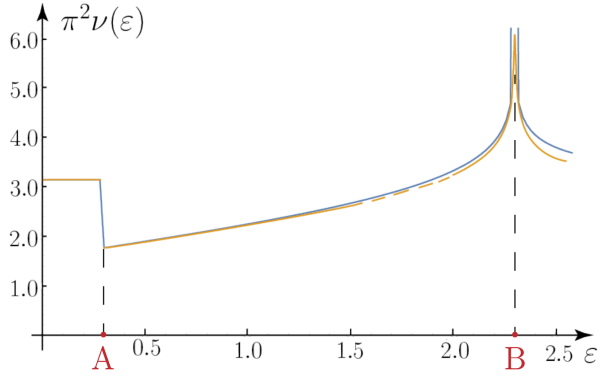


FIG. 3. Comparison of the numerical DOS (blue curve) with analytical results (orange curve). The singularities of the function are clearly seen. At point  $A = \Delta_1 - \Delta$  DOS function has a jump (Eq. (14a)) and at point  $B = \Delta_1 + \Delta$ , DOS has a logarithmic divergence (Eq. (13)). We used  $\Delta = 1$ (a.u.) is the Peierls energy gap and  $\Delta_1 = 1.3$ (a.u.) is the antinesting term.

A):

$$\begin{aligned} \nu(\Delta_1 - \Delta + \delta\varepsilon) &= \\ \frac{1}{2\pi v_F b} \left[ [1 - f(\delta\varepsilon)] + f(\delta\varepsilon)\theta(-\delta\varepsilon) \right], \quad \Delta < \Delta_1 \quad (14a) \\ \nu(\Delta - \Delta_1 + \delta\varepsilon) &= \frac{1}{2\pi v_F b} f(-\delta\varepsilon)\theta(\delta\varepsilon), \quad \Delta > \Delta_1 \end{aligned} \quad (14b)$$

$$f(\delta\varepsilon) = \frac{1}{2} \sqrt{\frac{\Delta}{\Delta_1}} - \frac{\delta\varepsilon}{16} \sqrt{\frac{\Delta}{\Delta_1}} \frac{3\Delta_1 + \Delta}{\Delta_1},$$

The resulting graph, juxtaposing the analytical formulas (13)-(14b) in the vicinity of singularities and numerical

computation of (12) are presented in fig. (3).

### C. $T_c$ temperature

Now we analyze how the discussed above singular behavior of DOS and the antinesting term affect the superconducting transition temperature  $T_c$  on DW background.

The equation for  $T_c$  is given by the BCS integral [78]

$$\frac{2}{g} = 2 \int_0^{\omega_D} \frac{d\xi}{\xi} \tanh \frac{\xi}{2T_c} \nu(\xi), \quad (15)$$

where  $g$  is the electron-phonon coupling constant in the BCS theory and  $\omega_D$  is the cutoff at Debye frequency. The Eq. (15) reproduces the corresponding integral derived from the linearized Gor'kov equations for superconductivity on the DW background [71, 82]).

We perform the calculation at Debye frequency  $\omega_D < \Delta_1 + \Delta$ . i.e. the integration domain doesn't include the log-singularity of the DOS. This can be the case in e.g. rare earth tellurides ( $\sim 170$  K)[83], where  $\omega_D \sim 0.015$  eV. The superconductive gap is assumed to vanish, since we position ourselves just above the transition temperature. In this case the integration (15) can be performed analytically with the help of expression (14a). We obtain the following analytical result for  $T_c$ :

$$\begin{aligned} T_c &= \left( \frac{\omega_D}{\Delta_1 - \Delta} \right)^{-\frac{\delta\nu}{\nu}} T_0, \\ T_0 &= \omega_D e^{-\frac{1}{\nu g}}, \quad \nu = \frac{1}{\pi v_F b}, \quad \delta\nu = \frac{1}{\pi v_F b} \sqrt{\frac{\Delta}{\Delta_1}} \end{aligned} \quad (16)$$

We expectedly reproduced the nonanalytic exponential  $\nu$  - dependence of the  $T_c$ . However, we also see an interesting change in the pre-exponential part. This is precisely where the antineesting term in the initial Hamiltonian (3) comes on stage. The comparison of the analytical result (16) with numerical calculation of integral (15) is presented in Fig. 4. Formulae (16) and the plot in Fig. 4 are the main physical results of this section.

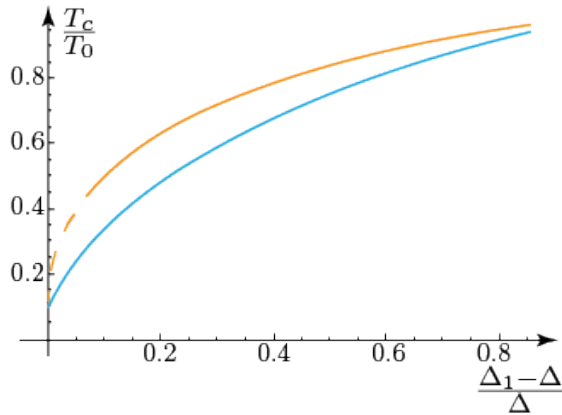


FIG. 4. Comparison of the numerical  $T_c$  (blue curve) with analytical result (16) (orange curve), where  $\Delta_1$  is the antineesting term and  $\Delta$  is the Peierls energy gap. The dashed part of the analytical curve corresponds to the region  $\Delta_1 - \Delta \lesssim T_c$  where the analytical relation (16) doesn't work.

#### IV. CONDUCTIVITY

In this section we present the computation of conductivity given by the integral obtained from the Kubo' formula in the DW state described within the mean-field approximation

$$\sigma_{ij} = - \int \frac{d\varepsilon}{2\pi} \frac{\partial f(\varepsilon)}{\partial \varepsilon} \int \frac{d^2\mathbf{k}}{(2\pi)^2} v_i(\mathbf{k}) v_j(\mathbf{k}) G^A(\varepsilon, \mathbf{k}) G^R(\varepsilon, \mathbf{k}), \quad (17)$$

where  $f(\varepsilon)$  is the Fermi distribution function and  $v_i(\mathbf{k}) \equiv \nabla_{k_i} E(\mathbf{k})$  is  $i$ th component of the velocity vector operator (see Eq.10).

The impurity-electron scattering rate is given by the imaginary part of the quasiparticle Green's function self-energy:

$$\frac{1}{2\tau} = \pi n_{imp} \int \delta(E(\mathbf{k})) \frac{d^2\mathbf{k}}{(2\pi)^2} = \pi n_{imp} g^2 \nu(0). \quad (18)$$

Integrating (17) over energy  $\varepsilon$ , yields the following expressions for conductivity tensor:

$$\begin{aligned} \sigma_{xx}(T) &= \frac{\tau}{2T} \int \xi(\mathbf{k}, T) \frac{d\mathbf{k}}{(2\pi)^2} \\ \sigma_{yy}(T) &= \frac{\tau}{2T} \int [2t_y \sin bp_y]^2 \xi(\mathbf{k}, T) \frac{d\mathbf{k}}{(2\pi)^2}, \end{aligned} \quad (19)$$

with

$$\xi(\mathbf{k}, T) = \frac{1}{4 \cosh^2 \frac{E(\mathbf{k}, T)}{2T}} \frac{(v_F k_x - t_y \cos bk_y)^2}{(v_F p_x - t_y \cos bk_y)^2 + \Delta^2(T)}. \quad (20)$$

The temperature dependence of the Peierls gap  $\Delta$  is taken in the mean-field approximation and Landau theory of the second-order phase transition as:

$$\Delta(T) = \Delta_0 \sqrt{1 - \frac{T}{T_c}}. \quad (21)$$

Next, we need to keep in mind that apart from impurity scattering there is an additional contribution to the electron scattering rate from electron-phonon interaction, the full scattering rate being the algebraic sum of the impurity and phonon scattering.

As is known, the electron-phonon interaction is described by the Bloch-Gruneisen law [79]

$$\begin{aligned} \frac{1}{\tau} &= A \cdot F\left(\frac{\theta_D}{T}\right), \\ F(z) &= \int_0^z \frac{z^5 dz}{(e^z - 1)(1 - e^{-z})}. \end{aligned} \quad (22)$$

Here the constant  $A$  contains the sound velocity, the ion mass and Debye temperature  $\theta_D$ .

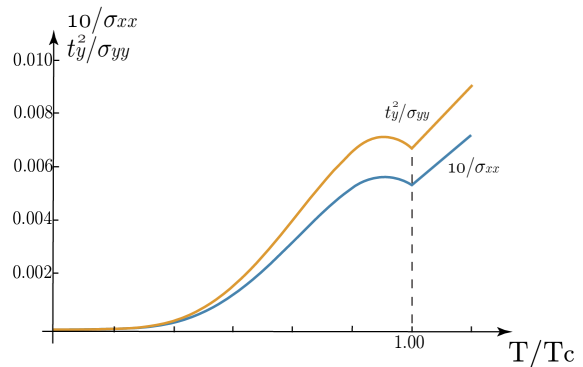


FIG. 5. Numerical resistivity  $1/\sigma_{xx}$  (blue curve) and  $1/\sigma_{yy}$  (orange curve) as a functions of temperature. Parameter  $A$  entering the scattering rate (22) is taken such that the residual resistance ratio parameter for  $\sigma_{xx}$  is  $\approx 70$ .

Numerical integration of Eq. (19) and the resultant conductivities are presented in Fig. (5). To perform calculations, we took realistic DW parameters [52]  $\Delta_0 = 0.27$  eV,  $T_c = 0.03$  eV,  $t_y = 0.37$  eV,  $t'_y = 0.16$  eV. Our results presented by plots in Fig. 5 demonstrate a qualitative consistency with the experimental data obtained in paper [52] and with numerous other experimental curves [27, 28]. This is the second main result of our paper.

## V. DISCUSSION

We studied the influence of the CDW with arbitrarily imperfect nesting on the critical temperature of the superconducting transition for the general model of a realistic quasi-1D metal. We have discovered that the imperfect nesting manifests itself in the strong renormalization of the preexponential factor in the dependence of BCS critical temperature on the electron DOS.

The discussed renormalization comes from the change in the electron dispersion and in the FS geometry due to the antinesting term  $t'_y$  in the Hamiltonian (3).

Here, the following important remark is in order. In the main body of the paper we completely discarded the influence of the antinesting term  $t'_y$  on the nesting vector  $\mathbf{Q}$ . Now we need to elaborate on this. Strictly speaking, at finite  $t'_y$  the Fermi surface loses the perfect nesting property. Inevitably, the question arises if the ideal nesting vector  $Q = (2k_F, \pi/b)$  can be used as a principal vector for the CDW formation. One could even ask if the introduction of such a vector was still meaningful in the absence of the FS nesting. The meaning of  $\mathbf{Q}$  in the absence of ideal nesting is indeed different. It should be interpreted as the displacement vector that maximizes the Kubo susceptibility

$$\chi(T, \mathbf{Q}) = - \int \frac{d\mathbf{k}}{(2\pi)^2} \frac{n_F(\mathbf{k} - \mathbf{Q}, T) - n_F(\mathbf{k}, T)}{\epsilon(\mathbf{k} - \mathbf{Q}) - \epsilon(\mathbf{k})}, \quad (23)$$

since the condition of the Peierls transition corresponds to the equation  $\chi(\mathbf{Q}) = g^{-1}$ , where  $g$  is the electron-phonon coupling constant and  $n_F(\mathbf{k}, T)$  is the Fermi distribution function. Taking a realistic temperature  $T = 100K$ , we computed the displacement  $\delta\mathbf{Q}$  of the CDW wave vector. Our calculation gives  $\delta Q_x/Q_x \approx -0.02$  and  $\delta Q_y/Q_y \approx -0.2$  in a reasonable agreement with earlier calculations. The corresponding numerical plot of the DoS, where the correct displacement vector  $\mathbf{Q}$  is taken into account, is presented in Fig. 6. As we see from Fig. 6, the positions of singularities and the quantitative shape of the curve are not significantly affected by the change of the nesting vector  $\delta\mathbf{Q}$ . This way one sees that for not too large antinesting term, the contribution to the DOS from the change of  $Q$  is negligible.

Finally, the temperature dependence of the conductivity tensor is analyzed in the framework of our model. We show that the nontrivial DOS leads to qualitative agreement of our results and the experimental data in rare-earth tritellurides [52] and in many other DW compounds [27, 28].

- 
- [1] J. Chang, E. Blackburn, A.T. Holmes, N.B. Christensen, J. Larsen, J. Mesot, Ruixing Liang, D.A. Bonn, W.N. Hardy, A. Watenphul, M.v. Zimmermann, E.M. Forgan, and S.M. Hayden. Direct observation of competition between superconductivity and charge density wave order in YBa2Cu3O6.67. *Nature Phys*, 8(12):871–876, October 2012.
- [2] S. Blanco-Canosa, A. Frano, T. Loew, Y. Lu, J. Porras, G. Ghiringhelli, M. Minola, C. Mazzoli, L. Braicovich, E. Schierle, E. Weschke, M. Le Tacon, and B. Keimer. Momentum-dependent charge correlations in YBa2Cu3O6+ $\delta$  Superconductors probed by resonant x-ray scattering: Evidence for three competing phases. *Phys. Rev. Lett.*, 110(18):187001, May 2013.
- [3] W. Tabis, B. Yu, I. Bialo, M. Bluschke, T. Kolodziej, A. Kozłowski, E. Blackburn, K. Sen, E.M. Forgan, M.v. Zimmermann, Y. Tang, E. Weschke, B. Vignolle, M. Heping, H. Gretarsson, R. Sutarto, F. He, M. Le Tacon, N. Barišić, G. Yu, and M. Greven. Synchrotron x-ray scattering study of charge-density-wave order in HgBa2CuO4+ $\delta$ . *Phys. Rev. B*, 96(13):134510, October 2017.
- [4] W. Tabis, Y. Li, M. Le Tacon, L. Braicovich, A. Kreyssig, M. Minola, G. Dellea, E. Weschke, M. J. Veit, M. Ramazanoglu, A. I. Goldman, T. Schmitt, G. Ghiringhelli, N. Barišić, M. K. Chan, C. J. Dorow, G. Yu, X. Zhao, B. Keimer, and M. Greven. Charge order and its connection with fermi-liquid charge transport in a pristine

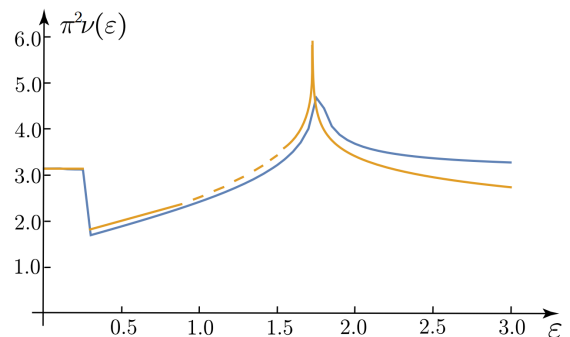


FIG. 6. Comparison of the numerical DOS (blue curve) with analytical result (orange curve) with correct DW vector  $\mathbf{Q}$ . The general view of the DOS function is not changed (see Fig. 3 for comparison).

high- $t_c$  cuprate. *Nature Communications*, 5(1):5875, Dec 2014.

- [5] Eduardo H. da Silva Neto, Riccardo Comin, Feizhou He, Ronny Sutarto, Yeping Jiang, Richard L. Greene, George A. Sawatzky, and Andrea Damascelli. Charge ordering in the electron-doped superconductor Nd<sub>2-x</sub>Ce<sub>x</sub>CuO<sub>4</sub>. *Science*, 347(6219):282–285, 2015.
- [6] J.-J. Wen, H. Huang, S.-J. Lee, H. Jang, J. Knight, Y. S. Lee, M. Fujita, K. M. Suzuki, S. Asano, S. A.

- Kivelson, C.-C. Kao, and J.-S. Lee. Observation of two types of charge-density-wave orders in superconducting  $\text{La}_{2-x}\text{Sr}_x\text{CuO}_4$ . *Nature Communications*, 10(1):3269, Jul 2019.
- [7] S. Medvedev, T. M. McQueen, I. A. Troyan, T. Palasyuk, M. I. Eremets, R. J. Cava, S. Naghavi, F. Casper, V. Ksenofontov, G. Wortmann, and C. Felser. Electronic and magnetic phase diagram of  $\beta\text{-Fe}_1.01\text{Se}$  with superconductivity at 36.7 K under pressure. *Nature Materials*, 8(8):630–633, Aug 2009.
- [8] Qimiao Si, Rong Yu, and Elihu Abrahams. High-temperature superconductivity in iron pnictides and chalcogenides. *Nat Rev Mater*, 1(4):16017, March 2016.
- [9] Xu Liu, Lin Zhao, Shaolong He, Junfeng He, Defa Liu, Daixiang Mou, Bing Shen, Yong Hu, Jianwei Huang, and X J Zhou. Electronic structure and superconductivity of FeSe-related superconductors. *J. Phys.: Condens. Matter*, 27(18):183201, April 2015.
- [10] M K Wu, P M Wu, Y C Wen, M J Wang, P H Lin, W C Lee, T K Chen, and C C Chang. An overview of the Fe-chalcogenide superconductors. *Journal of Physics D: Applied Physics*, 48(32):323001, Jul 2015.
- [11] Chao-Sheng Lian, Chen Si, and Wenhui Duan. Unveiling charge-density wave, superconductivity, and their competitive nature in two-dimensional NbSe<sub>2</sub>. *Nano Lett.*, 18(5):2924–2929, April 2018.
- [12] Kyuil Cho, M. Kończykowski, S. Teknowijoyo, M.A. Tanatar, J. Guss, P.B. Gartin, J.M. Wilde, A. Kreyssig, R.J. McQueeney, A.I. Goldman, V. Mishra, P.J. Hirschfeld, and R. Prozorov. Using controlled disorder to probe the interplay between charge order and superconductivity in NbSe<sub>2</sub>. *Nat Commun*, 9(1):2796, July 2018.
- [13] Liwen Feng, Jiayuan Cao, Tim Priessnitz, Yunyun Dai, Thales de Oliveira, Jiayu Yuan, Ryosuke Oka, Min-Jae Kim, Min Chen, Alexey N. Ponomaryov, Igor Ilyakov, Haotian Zhang, Yongbo Lv, Valentina Mazzotti, Gideok Kim, Georg Christiani, Gennady Logvenov, Dong Wu, Yuan Huang, Jan-Christoph Deinert, Sergey Kovalev, Stefan Kaiser, Tao Dong, Nanlin Wang, and Hao Chu. Dynamical interplay between superconductivity and charge density waves: A nonlinear terahertz study of coherently driven  $2h\text{-NbSe}_2$ . *Phys. Rev. B*, 108:L100504, Sep 2023.
- [14] Alla Chikina, Alexander Fedorov, Dilipkumar Bhoi, Vladimir Voroshnin, Erik Haubold, Yevhen Kushnirenko, Kee Hoon Kim, and Sergey Borisenko. Turning charge-density waves into Cooper pairs. *npj Quantum Materials*, 5(1):22, Apr 2020.
- [15] Lingyong Zeng, Xunwu Hu, Ningning Wang, Jianping Sun, Pengtao Yang, Mebrouka Boubeche, Shaojuan Luo, Yiyi He, Jinguang Cheng, Dao-Xin Yao, and Huixia Luo. Interplay between charge-density-wave, superconductivity, and ferromagnetism in  $\text{CuIr}_2\text{-xR}_x\text{Te}_4$  chalcogenides. *The Journal of Physical Chemistry Letters*, 13(10):2442–2451, Mar 2022.
- [16] Takehiko Ishiguro, Kunihiro Yamaji, and Gunzi Saito. *Organic Superconductors*. Springer Berlin Heidelberg, 1998.
- [17] Andrei Lebed, editor. *The Physics of Organic Superconductors and Conductors*. Springer Berlin Heidelberg, 2008.
- [18] D. Andres, M. V. Kartsovnik, W. Biberacher, K. Neumaier, E. Schuberth, and H. Müller. Superconductivity in the charge-density-wave state of the organic metal  $\alpha\text{-(BEDT-TTF)}_2\text{K}_2\text{Hg}(\text{SCN})_4$ . *Phys. Rev. B*, 72(17):174513, November 2005.
- [19] I. J. Lee, P. M. Chaikin, and M. J. Naughton. Critical field enhancement near a superconductor-insulator transition. *Phys. Rev. Lett.*, 88(20):207002, May 2002.
- [20] T. Vuletić, P. Auban-Senzier, C. Pasquier, S. Tomić, D. Jérôme, M. Héritier, and K. Bechgaard. Coexistence of superconductivity and spin density wave orderings in the organic superconductor  $(\text{TMTSF})_2\text{PF}_6$ . *Eur. Phys. J. B*, 25(3):319–331, February 2002.
- [21] N. Kang, B. Salameh, P. Auban-Senzier, D. Jerome, C. R. Pasquier, and S. Brazovskii. Domain walls at the spin-density-wave endpoint of the organic superconductor  $(\text{TMTSF})_2\text{PF}_6$  under pressure. *Phys. Rev. B*, 81(10):100509(R), March 2010.
- [22] Arjun Narayanan, Anshika Kiswandhi, David Graf, James Brooks, and Paul Chaikin. Coexistence of spin density waves and superconductivity in  $(\text{TMTSF})_2\text{PF}_6$ . *Phys. Rev. Lett.*, 112(14):146402, April 2014.
- [23] Ya. A. Gerasimenko, S. V. Sanduleanu, V. A. Prudkoglyad, A. V. Kornilov, J. Yamada, J. S. Qualls, and V. M. Pudalov. Coexistence of superconductivity and spin-density wave in  $(\text{TMTSF})_2\text{ClO}_4$ : Spatial structure of the two-phase state. *Phys. Rev. B*, 89(5):054518, February 2014.
- [24] Shingo Yonezawa, Claire A. Marrache-Kikuchi, Klaus Bechgaard, and Denis Jerome. Crossover from impurity-controlled to granular superconductivity in  $(\text{TMTSF})_2\text{ClO}_4$ . *Phys. Rev. B*, 97(1):014521, January 2018.
- [25] A M Gabovich, A I Voitenko, J F Annett, and M Ausloos. Charge- and spin-density-wave superconductors. *Supercond. Sci. Technol.*, 14(4):R1–R27, March 2001.
- [26] A. M. Gabovich, A. I. Voitenko, and M. Ausloos. Charge- and spin-density waves in existing superconductors: Competition between Cooper pairing and Peierls or excitonic instabilities. *Phys. Rep.*, 367(6):583–709, September 2002.
- [27] Pierre Monceau. Electronic crystals: An experimental overview. *Adv. Phys.*, 61(4):325–581, August 2012.
- [28] George Grüner. *Density Waves in Solids*. Addison-Wesley Pub. Co., Advanced Book Program, 1994.
- [29] V Kresin, Y Ovchinnikov, and S Wolf. Inhomogeneous superconductivity and the “pseudogap” state of novel superconductors. *Phys. Rep.*, 431(5):231–259, September 2006.
- [30] Seidali S. Seidov, Vladislav D. Kochev, and Pavel D. Grigoriev. First-order phase transition between superconducting and charge/spin density wave states causes their coexistence in organic metals. *Phys. Rev. B*, 108:125123, Sep 2023.
- [31] G. Campi, A. Bianconi, N. Poccia, G. Bianconi, L. Barba, G. Arrighetti, D. Innocenti, J. Karpinski, N. D. Zhigadlo, S. M. Kazakov, M. Burghammer, M. v. Zimmermann, M. Sprung, and A. Ricci. Inhomogeneity of charge-density-wave order and quenched disorder in a high- $T_c$  superconductor. *Nature*, 525(7569):359–362, Sep 2015.
- [32] Jennifer E Hoffman. Spectroscopic scanning tunneling microscopy insights into Fe-based superconductors. *Reports on Progress in Physics*, 74(12):124513, Nov 2011.
- [33] K. M. Lang, V. Madhavan, J. E. Hoffman, E. W. Hudson, H. Eisaki, S. Uchida, and J. C. Davis. Imaging the granular structure of high- $T_c$  superconductivity in underdoped

- Bi<sub>2</sub>Sr<sub>2</sub>CaCu<sub>2</sub>O<sub>8</sub>+ $\delta$ . *Nature*, 415(6870):412–416, January 2002.
- [34] W. D. Wise, Kamalesh Chatterjee, M. C. Boyer, Takeshi Kondo, T. Takeuchi, H. Ikuta, Zhijun Xu, Jinsheng Wen, G. D. Gu, Yayu Wang, and E. W. Hudson. Imaging nanoscale fermi-surface variations in an inhomogeneous superconductor. *Nature Phys*, 5(3):213–216, January 2009.
- [35] F. Masee, Y. Huang, R. Huisman, S. de Jong, J. B. Goedkoop, and M. S. Golden. Nanoscale superconducting-gap variations and lack of phase separation in optimally doped bafe<sub>1.86</sub>co<sub>0.14</sub>as<sub>2</sub>. *Phys. Rev. B*, 79:220517, Jun 2009.
- [36] Krzysztof Gofryk, Minghu Pan, Claudia Cantoni, Bayrammurad Saparov, Jonathan E. Mitchell, and Athena S. Sefat. Local inhomogeneity and filamentary superconductivity in pr-DopedCaFe<sub>2</sub>As<sub>2</sub>. *Phys. Rev. Lett.*, 112(4):047005, January 2014.
- [37] D. Cho, K. M. Bastiaans, D. Chatzopoulos, G. D. Gu, and M. P. Allan. A strongly inhomogeneous superfluid in an iron-based superconductor. *Nature*, 571(7766):541–545, Jul 2019.
- [38] Anton Fente, Alexandre Correa-Orellana, Anna E. Bohmer, Andreas Kreyssig, S. Ran, Sergey L. Budko, Paul C. Canfield, Federico J. Mompean, Mar García-Hernández, Carmen Munuera, Isabel Guillamón, and Hermann Suderow. Direct visualization of phase separation between superconducting and nematic domains in co-doped CaFe<sub>2</sub>As<sub>2</sub> close to a first-order phase transition. *Phys. Rev. B*, 97(1):014505, January 2018.
- [39] Can-Li Song, Yi-Lin Wang, Ye-Ping Jiang, Lili Wang, Ke He, Xi Chen, Jennifer E. Hoffman, Xu-Cun Ma, and Qi-Kun Xue. Suppression of superconductivity by twin boundaries in fese. *Phys. Rev. Lett.*, 109:137004, Sep 2012.
- [40] Yu. G. Naidyuk, G. Fuchs, D. A. Chareev, and A. N. Vasiliev. Doubling of the critical temperature of FeSe observed in point contacts. *Phys. Rev. B*, 93(14):144515, April 2016.
- [41] Ienari Iguchi, Tetsuji Yamaguchi, and Akira Sugimoto. Diamagnetic activity above  $t_c$  as a precursor to superconductivity in la<sub>2</sub>-xsrxcuo<sub>4</sub> thin films. *Nature*, 412(6845):420–423, Jul 2001.
- [42] Akira Sugimoto, Ienari Iguchi, Takashi Miyake, and Hisashi Sato. Diamagnetic precursor state in high- $t_c$  oxide superconductors near optimal doping using scanning superconducting quantum interference device microscopy. *Japanese Journal of Applied Physics*, 41:L497, May 2002.
- [43] A. A. Sinchenko, P. D. Grigoriev, A. P. Orlov, A. V. Frolov, A. Shakin, D. A. Chareev, O. S. Volkova, and A. N. Vasiliev. Gossamer high-temperature bulk superconductivity in FeSe. *Phys. Rev. B*, 95(16):165120, April 2017.
- [44] S. S. Seidov, K. K. Kesharpu, P. I. Karpov, and P. D. Grigoriev. Conductivity of anisotropic inhomogeneous superconductors above the critical temperature. *Phys. Rev. B*, 98(1):014515, July 2018.
- [45] Kaushal K. Kesharpu, Vladislav D. Kochev, and Pavel D. Grigoriev. Evolution of shape and volume fraction of superconducting domains with temperature and anion disorder in (tmtsf)<sub>2</sub>clo<sub>4</sub>. *Crystals*, 11(1), 2021.
- [46] Vladislav D. Kochev, Kaushal K. Kesharpu, and Pavel D. Grigoriev. Anisotropic zero-resistance onset in organic superconductors. *Phys. Rev. B*, 103:014519, Jan 2021.
- [47] Vladislav D. Kochev, Seidali S. Seidov, and Pavel D. Grigoriev. On the size of superconducting islands on the density-wave background in organic metals. *Magnetochemistry*, 9(7), 2023.
- [48] Pavel D. Grigoriev, Vladislav D. Kochev, Andrey P. Orlov, Aleksei V. Frolov, and Alexander A. Sinchenko. Inhomogeneous superconductivity onset in fese studied by transport properties. *Materials*, 16(5), 2023.
- [49] S Brazovskii and N Kirova. Electron selflocalization and superstructures in quasi one-dimensional dielectrics. *Sov. Sci. Rev. A*, 5:99–166, 1984.
- [50] L. P Gor'kov and P. D Grigoriev. Soliton phase near antiferromagnetic quantum critical point in Q1D conductors. *Europhys. Lett.*, 71(3):425–430, August 2005.
- [51] P. D. Grigoriev. Superconductivity on the density-wave background with soliton-wall structure. *Physica B*, 404(3-4):513–516, March 2009.
- [52] A. A. Sinchenko, P. D. Grigoriev, P. Lejay, and P. Monceau. Spontaneous breaking of isotropy observed in the electronic transport of rare-earth tritellurides. *Phys. Rev. Lett.*, 112:036601, Jan 2014.
- [53] K. Levin, D. L. Mills, and S. L. Cunningham. Incompatibility of bcs pairing and the peierls distortion in one-dimensional systems. i. mean-field theory. *Phys. Rev. B*, 10:3821–3831, Nov 1974.
- [54] C. A. Balseiro and L. M. Falicov. Superconductivity and charge-density waves. *Phys. Rev. B*, 20:4457–4464, Dec 1979.
- [55] Yu.A. Bychkov, L.P. Gor'kov, and I.E. Dzyaloshinskii. Possibility of superconductivity type phenomena in a one-dimensional system. *Sov. Phys. JETP*, 23:489, 1966.
- [56] Yuxuan Wang and Andrey Chubukov. Quantum-critical pairing in electron-doped cuprates. *Phys. Rev. B*, 88:024516, Jul 2013.
- [57] Y. Tanaka and K. Kuroki. Microscopic theory of spin-triplet  $f$ -wave pairing in quasi-one-dimensional organic superconductors. *Phys. Rev. B*, 70:060502, Aug 2004.
- [58] J. C. Nickel, R. Duprat, C. Bourbonnais, and N. Dupuis. Triplet superconducting pairing and density-wave instabilities in organic conductors. *Phys. Rev. Lett.*, 95:247001, Dec 2005.
- [59] L. P. Gor'kov and P. D. Grigoriev. Nature of the superconducting state in the new phase in(TMTSF)<sub>2</sub>PF<sub>6</sub>under pressure. *Phys. Rev. B*, 75(2):020507(R), January 2007.
- [60] F. Schmitt, P. S. Kirchmann, U. Bovensiepen, R. G. Moore, L. Rettig, M. Krenz, J.-H. Chu, N. Ru, L. Perfetti, D. H. Lu, M. Wolf, I. R. Fisher, and Z.-X. Shen. Transient electronic structure and melting of a charge density wave in tbte<sub>3</sub>. *Science*, 321(5896):1649–1652, 2008.
- [61] R. G. Moore, V. Brouet, R. He, D. H. Lu, N. Ru, J.-H. Chu, I. R. Fisher, and Z.-X. Shen. Fermi surface evolution across multiple charge density wave transitions in erte<sub>3</sub>. *Phys. Rev. B*, 81:073102, Feb 2010.
- [62] J.-S. Kang, C. G. Olson, Y. S. Kwon, J. H. Shim, and B. I. Min. Charge-density wave gap and  $ce$   $4f$  states in Cete<sub>2</sub> observed by photoemission spectroscopy. *Phys. Rev. B*, 74:085115, Aug 2006.
- [63] D. Qian, D. Hsieh, L. Wray, Y. Xia, R.J. Cava, E. Morosan, and M.Z. Hasan. Evolution of low-lying states in a doped cdw superconductor cuxtise<sub>2</sub>. *Physica B: Condensed Matter*, 403(5):1002–1004, 2008.



- [64] Hyejin Ryu, Yi Chen, Heejung Kim, Hsin-Zon Tsai, Shujie Tang, Juan Jiang, Franklin Liou, Salman Kahn, Caihong Jia, Arash A. Omrani, Ji Hoon Shim, Zahid Hussain, Zhi-Xun Shen, Kyoo Kim, Byung Il Min, Choongyu Hwang, Michael F. Crommie, and Sung-Kwan Mo. Persistent charge-density-wave order in single-layer tase2. *Nano Letters*, 18(2):689–694, Feb 2018.
- [65] Moritz Hoesch, Liam Gannon, Kenya Shimada, Benjamin J. Parrett, Matthew D. Watson, Timur K. Kim, Xiangde Zhu, and Cedimir Petrovic. Disorder quenching of the charge density wave in  $\text{zrte}_3$ . *Phys. Rev. Lett.*, 122:017601, Jan 2019.
- [66] H. Miao, G. Fabbris, R. J. Koch, D. G. Mazzone, C. S. Nelson, R. Acevedo-Esteves, G. D. Gu, Y. Li, T. Yilmaz, K. Kaznatcheev, E. Vescovo, M. Oda, T. Kurosawa, N. Momono, T. Assefa, I. K. Robinson, E. S. Bozin, J. M. Tranquada, P. D. Johnson, and M. P. M. Dean. Charge density waves in cuprate superconductors beyond the critical doping. *npj Quantum Materials*, 6(1):31, Mar 2021.
- [67] Hailan Luo, Qiang Gao, Hongxiong Liu, Yuhao Gu, Dingsong Wu, Changjiang Yi, Junjie Jia, Shilong Wu, Xiangyu Luo, Yu Xu, Lin Zhao, Qingyan Wang, Hanqing Mao, Guodong Liu, Zhihai Zhu, Youguo Shi, Kun Jiang, Jiangping Hu, Zuyan Xu, and X. J. Zhou. Electronic nature of charge density wave and electron-phonon coupling in kagome superconductor  $\text{kv}_3\text{sb}_5$ . *Nature Communications*, 13(1):273, Jan 2022.
- [68] Takemi Kato, Yongkai Li, Tappei Kawakami, Min Liu, Kosuke Nakayama, Zhiwei Wang, Ayumi Moriya, Kiyohisa Tanaka, Takashi Takahashi, Yugui Yao, and Takafumi Sato. Three-dimensional energy gap and origin of charge-density wave in kagome superconductor  $\text{kv}_3\text{sb}_5$ . *Communications Materials*, 3(1):30, May 2022.
- [69] Takemi Kato, Yongkai Li, Min Liu, Kosuke Nakayama, Zhiwei Wang, Seigo Souma, Miho Kitamura, Koji Horiba, Hiroshi Kumigashira, Takashi Takahashi, Yugui Yao, and Takafumi Sato. Surface-termination-dependent electronic states in kagome superconductors  $\text{AV}_3\text{sb}_5$  ( $a = \text{K}, \text{Rb}, \text{Cs}$ ) studied by micro-arpes. *Phys. Rev. B*, 107:245143, Jun 2023.
- [70] Alla Chikina, Henriette Lund, Marco Bianchi, Davide Curcio, Kirstine J. Dalgaard, Martin Bremholm, Shiming Lei, Ratnadwip Singha, Leslie M. Schoop, and Philip Hofmann. Charge density wave generated fermi surfaces in  $\text{ndte}_3$ . *Phys. Rev. B*, 107:L161103, Apr 2023.
- [71] PD Grigoriev. Properties of superconductivity on a density wave background with small ungapped fermi surface parts. *Physical Review B*, 77(22):224508, 2008.
- [72] Denis Jerome and Claude Bourbonnais. Quasi one-dimensional organic conductors: from Fröhlich conductivity and Peierls insulating state to magnetically-mediated superconductivity, a retrospective. *Comptes Rendus. Physique*, 25:17–178, 2024.
- [73] V. Brouet, W. L. Yang, X. J. Zhou, Z. Hussain, R. G. Moore, R. He, D. H. Lu, Z. X. Shen, J. Laverock, S. B. Dugdale, N. Ru, and I. R. Fisher. Angle-resolved photoemission study of the evolution of band structure and charge density wave properties in  $\text{rte}_3$  ( $r = \text{Y}, \text{La}, \text{Ce}, \text{Sm}, \text{Gd}, \text{Tb}, \text{and Dy}$ ). *Phys. Rev. B*, 77:235104, Jun 2008.
- [74] Abhishek Pathak, Mayanak K. Gupta, Ranjan Mittal, and Dipanshu Bansal. Orbital- and atom-dependent linear dispersion across the fermi level induces charge density wave instability in  $\text{eute}_4$ . *Phys. Rev. B*, 105:035120, Jan 2022.
- [75] Chen Zhang, Qi-Yi Wu, Ya-Hua Yuan, Xin Zhang, Hao Liu, Zi-Teng Liu, Hong-Yi Zhang, Jiao-Jiao Song, Yin-Zou Zhao, Fan-Ying Wu, Shu-Yu Liu, Bo Chen, Xue-Qing Ye, Sheng-Tao Cui, Zhe Sun, Xiao-Fang Tang, Jun He, Hai-Yun Liu, Yu-Xia Duan, Yan-Feng Guo, and Jian-Qiao Meng. Angle-resolved photoemission spectroscopy study of charge density wave order in the layered semiconductor  $\text{eute}_4$ . *Phys. Rev. B*, 106:L201108, Nov 2022.
- [76] D S Inosov, V B Zabolotnyy, D V Evtushinsky, A A Kordyuk, B Büchner, R Follath, H Berger, and S V Borisenko. Fermi surface nesting in several transition metal dichalcogenides. *New Journal of Physics*, 10(12):125027, dec 2008.
- [77] H. Miao, R. Fumagalli, M. Rossi, J. Lorenzana, G. Seibold, F. Yakhov-Harris, K. Kummer, N. B. Brookes, G. D. Gu, L. Braicovich, G. Ghiringhelli, and M. P. M. Dean. Formation of incommensurate charge density waves in cuprates. *Phys. Rev. X*, 9:031042, Sep 2019.
- [78] Alekseĭ Abrikosov. *Fundamentals of the Theory of Metals*.
- [79] John M Ziman. *Principles of the Theory of Solids*. Cambridge university press, 1979.
- [80] Gor'kov, L.P. and Lebed', A.G. On the stability of the quasi-one-dimensional metallic phase in magnetic fields against the spin density wave formation. *J. Physique Lett.*, 45(9):433–440, 1984.
- [81] P. D. Grigoriev and D. S. Lyubshin. Phase diagram and structure of the charge-density-wave state in a high magnetic field in quasi-one-dimensional materials: A mean-field approach. *Phys. Rev. B*, 72:195106, Nov 2005.
- [82] L. P. Gor'kov and P. D. Grigoriev. Nature of the superconducting state in the new phase in  $(\text{TMTSF})_2\text{pf}_6$  under pressure. *Phys. Rev. B*, 75:020507, Jan 2007.
- [83] A Banerjee, Yejun Feng, DM Silevitch, Jiyang Wang, JC Lang, H-H Kuo, IR Fisher, and TF Rosenbaum. Charge transfer and multiple density waves in the rare earth tellurides. *Physical Review B*, 87(15):155131, 2013.

### Appendix A: DOS with imperfect nesting

From now on we put  $v_F = 1$ ,  $b = 1$  restoring them in the final formulae. In this section we investigate the imperfect nesting case. The dispersion (3) doesn't satisfy the perfect nesting condition  $\varepsilon(\mathbf{k}) + \varepsilon(\mathbf{k} + \mathbf{Q}) \sim 0$ . Therefore, accordingly (3) the spectrum for quasiparticles (9) has the following view:

$$E(q_y) = \frac{-4t'_y \cos 2q_y}{2} \pm \sqrt{\frac{(2q_x - 2t_y \cos q_y)^2}{4} + \Delta^2}, \quad (\text{A1})$$

with

$$q_x = k_x - k_F, \quad q_y = k_y \quad (\text{A2})$$

In all following calculations, the region of integration is the quarter of the Brillouin zone due to the symmetry of the gapped spectrum (A1).

Let us first, assume that the anti nesting term is not small and satisfies the condition:

$$2t'_y = \Delta_1 > \Delta. \quad (\text{A3})$$

The DOS is possible to compute analytically in the vicinity of  $\Delta + \Delta_1$ :  $\epsilon = \Delta + \Delta_1 + \delta\epsilon$ ,  $\delta\epsilon \ll \Delta$ . After integrating over  $q_x$  integral (11) becomes as follows:

$$2 \int_0^\pi \frac{\Delta + \delta\epsilon + \Delta_1(1 + \cos 2q_y)}{\sqrt{(\Delta + \delta\epsilon + \Delta_1(1 + \cos 2q_y))^2 - \Delta^2}} \frac{dq_y}{(2\pi)^2}. \quad (\text{A4})$$

Subtracting singular terms, we obtain:

$$2 \int_0^\pi \left[ \frac{b + 2 \cos^2 q_y}{\sqrt{(b + 2 \cos^2 q_y)^2 - b^2}} - \sqrt{\frac{b}{4}} \frac{1}{|\cos q_y|} \right] \frac{dq_y}{(2\pi)^2} + 2\sqrt{\frac{b}{2}} \int_0^\pi \frac{1}{\sqrt{2 \cos^2 q_y + a}} \frac{dq_y}{(2\pi)^2}, \quad (\text{A5})$$

$$b = \frac{\Delta}{\Delta_1}, \quad a = \frac{\delta\epsilon}{\Delta_1}.$$

The first part of the integral (A5) can be taken easily with the substitution:

$$t = \cos q_y, \quad dq_y = \frac{1}{\sqrt{1-t^2}} \quad (\text{A6})$$

$$2 \int_0^\pi \left[ \frac{b + 2 \cos^2 q_y}{\sqrt{(b + 2 \cos^2 q_y)^2 - b^2}} - \sqrt{\frac{b}{4}} \frac{1}{|\cos q_y|} \right] \frac{dq_y}{(2\pi)^2} = \int_0^1 \left[ \frac{2t}{\sqrt{1-t^2}\sqrt{b+t^2}} + \frac{b - \sqrt{b^2 + bt^2}}{t\sqrt{b+t^2}\sqrt{1-t^2}} \right] \frac{dt}{(2\pi)^2} = \frac{1}{(2\pi)^2} \int_0^1 \frac{dt}{t\sqrt{1-t^2}} \left[ \frac{b + 2t^2}{\sqrt{b+t^2}} - \sqrt{b} \right] = \frac{1}{2\pi^2} \left[ \arcsin \frac{1}{\sqrt{1+b}} - \frac{\sqrt{b}}{2} \ln \left( 1 + \frac{1}{b} \right) \right]. \quad (\text{A7})$$

The second part of the integral (A5) is

$$\frac{2}{(2\pi)^2} \sqrt{\frac{b}{2}} \int_0^{\frac{\pi}{2}} \frac{ds}{\sqrt{2 \sin^2 s + a}} = \frac{2}{(2\pi)^2} \sqrt{\frac{b}{2}} \left[ \int_0^{\frac{\pi}{2}} \left( \frac{ds}{\sqrt{2} \sin s} - \frac{ds}{\sqrt{2}s} \right) + \int_0^{\frac{\pi}{2}} \frac{ds}{\sqrt{2s^2 + a}} \right] = \frac{\sqrt{b}}{(2\pi)^2} \left( \ln 4\sqrt{2} - \ln \sqrt{a} \right) \quad (\text{A8})$$

$$s = q_y - \frac{\pi}{2}, \quad \frac{s}{q_y} \ll 1.$$

Summarizing (A7) and (A8), we have the final form of the DOS in the main body of the paper (13).

Now let's suppose that  $\varepsilon = \Delta_1 - \Delta + \delta\epsilon$ ,  $\delta\epsilon \ll \Delta$ . Two different occasions are here. If  $\delta\epsilon > 0$  or  $\delta\epsilon = 0$  pockets have not yet appeared and the integral (12) is

$$\int_0^{\arccos \sqrt{b + \frac{\delta\epsilon}{\Delta_1}}} \frac{a - b + 2 \cos^2 q_y}{\sqrt{(a - b + 2 \cos^2 q_y)^2 - b^2}} \frac{dq_y}{(2\pi)^2}, \quad (\text{A9})$$

$$b = \frac{\Delta}{\Delta_1}, \quad a = \frac{\delta\epsilon}{\Delta_1}.$$

When  $\delta\epsilon = 0$  it is nice to use the substitution  $t = \cos q_y$ :

$$\int_0^{\arccos \sqrt{b}} \frac{-b + 2 \cos^2 q_y}{\sqrt{(-b + 2 \cos^2 q_y)^2 - b^2}} \frac{dq_y}{(2\pi)^2} = \int_0^{\arccos \sqrt{b}} \frac{2 \cos^2 q_y - b}{2\sqrt{(\cos^2 q_y - b)(\cos^2 q_y)}} \frac{dq_y}{(2\pi)^2} = \int_{\sqrt{b}}^1 \frac{2t^2 - b}{2t\sqrt{(t^2 - b)\sqrt{1-t^2}}} \frac{dt}{(2\pi)^2} = \frac{1}{8\pi} \left( 1 - \frac{\sqrt{b}}{2} \right). \quad (\text{A10})$$

When  $\delta\epsilon < 0$ , two small pockets appear in the area of the point  $q_y = \pi/2$ . Consequently, pockets make a contribution in the DOS:

$$\int_{\frac{\pi}{2} - \arccos \frac{\sqrt{|a|}}{2}}^{\frac{\pi}{2}} \frac{a - b + 2 \cos^2 q_y}{\sqrt{(a - 2b + 2 \cos^2 q_y)(a + 2 \cos^2 q_y)}} \frac{dq_y}{(2\pi)^2} = \int_0^{\arcsin \frac{\sqrt{|a|}}{2}} \frac{-|a| - b + 2 \sin^2 s}{\sqrt{(-|a| - 2b + 2 \sin^2 s)(-|a| + 2 \sin^2 s)}} \frac{ds}{(2\pi)^2}, \quad (\text{A11})$$

$$s = q_y - \frac{\pi}{2}, \quad \frac{s}{q_y} \ll 1.$$

Next, we expand  $\sin s$  and  $\arcsin \frac{\sqrt{|a|}}{2}$  over small parameters:

$$\int_0^{\sqrt{\frac{|a|}{2}}} \frac{-|a| - b + 2s^2}{\sqrt{(-|a| - 2b + 2s^2)(-|a| + 2s^2)}} \frac{ds}{(2\pi)^2} = \int_0^{\sqrt{\frac{|a|}{2}}} \frac{-b}{\sqrt{2b(|a| - 2s^2)}} \frac{ds}{(2\pi)^2} = -\sqrt{b} \frac{1}{16\pi}. \quad (\text{A12})$$

Finally, combining Eq. (A10) and Eq. (A12) we obtain an equation for the density of states (14a) Now let us calculate the DOS with the energy  $\varepsilon = \Delta - \Delta_1 + \delta\varepsilon$ ,  $\Delta > \Delta_1$ . The integral of DOS (12) is

$$\int_0^{\pi/2} \frac{a + \frac{b}{2} - \sin q_y^2}{\sqrt{(a + b - \sin q_y^2)(a - \sin q_y^2)}} \frac{dq_y}{(2\pi)^2},$$

$$a = \frac{\delta\varepsilon}{2\Delta_1}, \quad b = \frac{\Delta}{\Delta_1}, \quad \sin q_y = a \sin t. \quad (\text{A13})$$

The completely analogous calculations yield Eq. 14b.

### Appendix B: SC critical temperature

Using equation for  $T_c$  (15):

$$\frac{2}{g} = 2 \int_0^{\omega_D} \frac{d\xi}{\xi} \tanh \frac{\xi}{2T_c} \nu(\xi) \quad (\text{B1})$$

The r.h.s. can be represented as the sum of simple integrals, where we use the step-like structure of the density

of states, presented in (14a), (14b).

$$\frac{1}{g} = \nu \int_{T_c}^{\Delta_1 - \Delta} \frac{dx}{x} + (\nu - \delta\nu) \int_{\Delta_1 - \Delta}^{\omega_D} \frac{dx}{x} =$$

$$\nu \ln \left( \frac{\Delta_1 - \Delta}{T_c} \right) + (\nu - \delta\nu) \ln \left( \frac{\omega_D}{\Delta_1 - \Delta} \right) =$$

$$\nu \ln \frac{\omega_D}{T_c} - \delta\nu \ln \frac{\omega_D}{\Delta_1 - \Delta}. \quad (\text{B2})$$

The equation over  $T_c$  (B2) is solved and gives

$$T_c = \omega_D \left( \frac{\omega_D}{\Delta_1 - \Delta} \right)^{-\frac{\delta\nu}{\nu}} e^{-\frac{1}{\nu g}},$$

$$\nu = \frac{1}{\pi v_F b}, \quad \delta\nu = \frac{1}{\pi v_F b} \sqrt{\frac{\Delta}{\Delta_1}}. \quad (\text{B3})$$

### Appendix C: Conductivity

The integral (17) is computed with complex analysis. Combination of Green functions

$$G^A(\varepsilon, \mathbf{k}) G^R(\varepsilon, \mathbf{k}) = \frac{1}{(\varepsilon - E(\mathbf{k}))^2 + \left(\frac{1}{2\tau}\right)^2} \quad (\text{C1})$$

can be substituted with the Dirac  $\delta$ -function  $\delta(\varepsilon - E(\mathbf{k}))$  in the limit  $\frac{1}{\tau} \ll \varepsilon - E(\mathbf{k})$ :

$$G^A(\varepsilon, \mathbf{k}) G^R(\varepsilon, \mathbf{k}) \approx \tau \delta(\varepsilon - E(\mathbf{k})). \quad (\text{C2})$$

After integrating over  $\varepsilon$ , Eq.(17) simplifies to

$$\sigma_{ij}(T) = \frac{\tau}{2T} \int \frac{d\mathbf{k}}{(2\pi)^2} \frac{1}{4 \cosh^2 \frac{E(\mathbf{k}, T)}{2T}} \frac{\partial E(\mathbf{k})}{\partial r_i} \frac{\partial E(\mathbf{k})}{\partial r_j}. \quad (\text{C3})$$

From the last equation we obtain the final Eqs. (19) presented in the main body.